ISSN 0140-3818

University of Southampton

School of Engineering Sciences

Ship Science

Boundary Layer Flow on a Long Thin Cylinder

O.R. Tutty, W.G. Price

Ship Science Report No. 120

October 2000

Boundary Layer Flow on a Long Thin Cylinder

O.R. Tutty W.G. Price

School of Engineering Sciences
University of Southampton
Southampton SO17 1BJ, UK

Introduction

In a classical analysis of the flow in an external boundary layer the pressure gradient is obtained from the inviscid (potential) solution for flow past the body. The simplest example is Blasius flow past a flat plate aligned with the flow in which the pressure gradient is zero. Consider the case of a circular cylinder with the external flow aligned along the cylinders axis. If the cylinder is solid, then the flow will adjust to the presence of the cylinder, generating a nonzero pressure gradient near the nose of the cylinder. However the pressure gradient will decay asymptotically along the cylinder. Alternatively, if fluid is being sucked into the cylinder at the free stream velocity, the pressure gradient will zero from the leading edge.

This problem, of flow developing along a circular cylinder with zero pressure gradient, is the one that will be considered here. There is little reported in the literature on this problem. Seban and Bond [1] give the first three terms in a series solution valid near the leading edge of the cylinder, giving in particular expressions for the shear stress on the surface and the displacement area. Kelly [2] presents different values for some of the coefficients in the Seban and Bond solution. In contrast, Stewartson [3] gives a series solution for very large distances along the cylinder. In [3] it is shown that sufficiently far along the cylinder, the wall shear stress decays logarithmically with distance, rather than than algebraically as is usually found. Glauert and Lighthill [4] considered the flow along the entire cylinder. They developed a similar series solution to Stewartson for the flow far downstream. Also, they developed an approximate solution for flow near the leading edge based on a Pohlhausen method with a logarithmic profile, and have shown that this solution produces reasonable agreement with different series solutions valid near the leading edge and far downstream. Using these solutions they produced a set of recommended curves for quantities such as the displacement area and the skin friction

Here a full numerical solution of the boundary layer problem will be presented and compared with with the previous results.

Formulation

Assuming zero pressure gradient, and the boundary layer equations in polar coordinates (x, r), non-dimensionalised on the cylinder radius, are

$$\frac{\partial u}{\partial x} + \frac{\partial v}{\partial r} + \frac{v}{r} = 0 \tag{1}$$

$$u\frac{\partial u}{\partial x} + v\frac{\partial u}{\partial r} = \frac{1}{Re}\left(\frac{\partial^2 u}{\partial r^2} + \frac{1}{r}\frac{\partial u}{\partial r}\right) \tag{2}$$

where (u, v) are the stream wise and radial velocity components, non-dimensionalised on the free stream velocity U_∞. $Re = U_\infty a/\nu$ is the Reynolds number where ν is the kinematic viscosity.

Introducing the transformation

$$y = (r-1)Re^{\frac{1}{2}}, \qquad v \to Re^{-\frac{1}{2}}v, \tag{3}$$

which incorporates the usual $Re^{-\frac{1}{2}}$ scaling, produces

$$\frac{\partial u}{\partial x} + \frac{\partial v}{\partial y} + \frac{vRe^{-\frac{1}{2}}}{1 + Re^{-\frac{1}{2}}y} = 0 \tag{4}$$

$$u\frac{\partial u}{\partial x} + v\frac{\partial u}{\partial y} = \frac{\partial^2 u}{\partial y^2} + \frac{Re^{-\frac{1}{2}}}{1 + Re^{-\frac{1}{2}}y}\frac{\partial u}{\partial y} \tag{5}$$

with boundary conditions

$$u = v = 0 \ \text{ at } \ y = 0 \tag{6}$$

$$u \to 1 \ \text{ as } \ y \to \infty \tag{7}$$

In addition a suitable initial condition must be specified. This will be considered below.

Theoretical Results

From (4-7) it may appear that the leading term in the boundary layer solution will be flat plate Blasius flow, with an $O(Re^{-\frac{1}{2}})$ perturbation. While this is true near the leading edge of the cylinder, further downstream this approximation beaks down. With the Blasius solution, y scales as $x^{\frac{1}{2}}$. Hence the ratio of the terms on the right side of (5) is

$$\frac{Re^{-\frac{1}{2}}}{1 + Re^{-\frac{1}{2}}y}\frac{\partial u}{\partial y}\Big/\frac{\partial^2 u}{\partial y^2} = O\left(\frac{Re^{-\frac{1}{2}}x^{\frac{1}{2}}}{1 + Re^{-\frac{1}{2}}x^{\frac{1}{2}}}\right) \tag{8}$$

Hence when $x = O(Re)$ the terms of the right side are of similar magnitude due to the growth in the boundary layer, and Blasius flow flow will not be the leading term in the solution when the boundary layer thickness becomes comparable with the cylinder radius. Further, at this stage it is also necessary to include the additional term in the continuity equation at leading order.

Here the extra term will be included from the leading edge by adopting the boundary layer equations in the form (4-7). These equations will be solved numerically, using the method outlined below. First, however, the first two term in the series solution for the flow near the leading edge, valid in the region $0 < x \ll Re$, will be presented. Following Seban and Bond, take

$$\eta = Re^{\frac{1}{2}} x^{-\frac{1}{2}} (r^2 - 1)/2, \qquad \xi = Re^{-\frac{1}{2}} x^{\frac{1}{2}} \tag{9}$$

and

$$\psi = Re^{-\frac{1}{2}} x^{\frac{1}{2}} f(\xi, \eta) \tag{10}$$

This gives

$$u = \frac{1}{r}\frac{\partial \psi}{\partial r} = \frac{\partial f}{\partial \eta}, \qquad v = -\frac{1}{r}\frac{\partial \psi}{\partial x} = -\frac{Re^{-\frac{1}{2}} x^{-\frac{1}{2}}}{r}\left[-\eta \frac{\partial f}{\partial \eta} + \frac{\partial}{\partial \xi}(\xi f)\right] \tag{11}$$

The governing equation for f is

$$\frac{\partial}{\partial \eta}\left[(1 + 2\xi\eta)\frac{\partial^2 f}{\partial \eta^2}\right] + \frac{1}{2} f \frac{\partial^2 f}{\partial \eta^2} + \frac{1}{2}\xi \left(\frac{\partial f}{\partial \xi}\frac{\partial^2 f}{\partial \eta^2} + \frac{\partial f}{\partial \eta}\frac{\partial^2 f}{\partial \eta \partial \xi}\right) = 0 \tag{12}$$

Taking

$$f = f_0(\eta) + \xi f_1(\eta) + \ldots \tag{13}$$

where it is assumed that $\xi \ll 1$, produces

$$f_0''' + \frac{1}{2} f_0 f_0'' = 0 \tag{14}$$

$$f_1''' + \frac{1}{2} f_0 f_1'' - \frac{1}{2} f_0' f_1' + f_0'' f_1 + 2\eta f_0''' + 2 f_0'' = 0 \tag{15}$$

The boundary conditions are

$$f_0(0) = f_0'(0) = 0 \quad \text{and} \quad f_0' \to 1 \text{ as } \eta \to \infty \tag{16}$$

$$f_1(0) = f_1'(0) = 0 \quad \text{and} \quad f_1' \to 0 \text{ as } \eta \to \infty \tag{17}$$

Equation (16) is the Blasius equation. The problems defined by (14-17) are easily solved numerically. The solution give the dimensionless skin friction $\tau = \partial u / \partial y$ as

$$\tau = 0.332 x^{-\frac{1}{2}} + 0.694 Re^{-\frac{1}{2}} + \ldots \tag{18}$$

This is essentially the same expression given by Seban and Bond/Kelly [1, 2], but with a small difference in the second coefficient, due presumably to the increased accuracy of the calculations performed here. Equation (18) has the skin friction tending to a constant for large x, although formally it is valid only for $x \ll Re$.

The asymptotic series produced by Glauert and Lighthill [4] for large x gives

$$\tau = \frac{2}{\delta} + \frac{2\gamma}{\delta^2} + \frac{2\gamma^2 - \frac{1}{2}\pi^2 - 4\ln 2}{\delta^3} + O(\delta^{-4}) \tag{19}$$

where $\gamma = 0.5772$ is Euler's constant and $\delta = \ln(4x/Re)$. This formula has τ decaying as x increases, albeit slowly, inversely with $\ln x$. Stewartson [3] produced a similar results, but used $\hat{\delta} = \ln(4x/ReC)$ in place of δ, where $\ln C = \gamma$. Stewartson's formula is

$$\tau = \frac{2}{\hat{\delta}} - \frac{\frac{1}{2}\pi^2 + 4\ln 2}{\hat{\delta}^3} + \ldots + \frac{Re}{2x}\frac{7}{\hat{\delta}} + \ldots \tag{20}$$

Equation (19) can be derived from Stewartson's expression by writing $\hat{\delta} = \delta - \gamma$ and expanding the first two terms in(20) for large x. The Glauert and Lighthill expression for τ is used here as it gives a better comparison with the numerical solutions presented below than Stewartson's formula.

Another of quantity of interest is the "displacement area", which represents the amount by which the fluid in the main stream is displaced by the action the viscous effects in the boundary layer. In two-dimensional flow the displacement thickness gives the distance which the streamlines in the far field are displaced from those of the inviscid flow past the body. However, in cylindrical coordinates, the displacement of the streamlines in away from the surface decays inversely with r due to the expansion in area with r. Hence there is no unique displacement thickness, and the appropriate quantity is the displacement area. In non-dimensional form

$$\Delta_1 = 2\int_1^\infty (1-u) r dr \tag{21}$$

gives the displacement area relative to the cross-sectional area of the cylinder. Substituting the Blasius profile directly into (21) produces

$$\Delta_1 = Re^{-\frac{1}{2}} x^{\frac{1}{2}} \left[3.44 + 4.37 Re^{-\frac{1}{2}} x^{\frac{1}{2}}\right] \tag{22}$$

The solution to (14-17) gives

$$\Delta_1 = Re^{-\frac{1}{2}} x^{\frac{1}{2}} \left[3.442 + 0.143 Re^{-\frac{1}{2}} x^{\frac{1}{2}} + \ldots\right] \tag{23}$$

Equation (23) is valid only for $0 < x \ll Re$. For large x Glauert and Lighthill give

$$\Delta_1 = \frac{4x}{Re}\left[\frac{1}{\delta} + \frac{1 + \gamma + 2\ln 2}{\delta^2} + \ldots\right] \tag{24}$$

Stewartson [3] states that the boundary layer thickness is ultimately of order $(x/Re\hat{\delta})^{\frac{1}{2}}$, consistent with (24). Hence the boundary layer grows at a factor $(\ln x)^{-\frac{1}{2}}$ more slowly than for the flat plate.

Numerical Method

In the original polar coordinates the velocity can be obtained from the streamfunction $\psi(x, r)$ through

$$u = \frac{1}{r}\frac{\partial \psi}{\partial r}, \quad v = -\frac{1}{r}\frac{\partial \psi}{\partial x} \tag{25}$$

In boundary layer coordinates write

$$\psi = Re^{-\frac{1}{2}}\Psi(x, z) \tag{26}$$

where $z = Re^{\frac{1}{2}}x^{-\frac{1}{2}}(r-1)$. The boundary layer equations (4) and (5) can now be written as a system of coupled first order differential equations:

$$u = \frac{x^{-\frac{1}{2}}}{1 + Re^{-\frac{1}{2}}x^{\frac{1}{2}}z}\frac{\partial \Psi}{\partial z} \tag{27}$$

$$\tau = x^{-\frac{1}{2}}\frac{\partial u}{\partial z} \tag{28}$$

$$u\frac{\partial u}{\partial x} - \frac{1}{1 + Re^{-\frac{1}{2}}x^{\frac{1}{2}}z}\frac{\partial \Psi}{\partial x}\tau = x^{-\frac{1}{2}}\frac{\partial \tau}{\partial z} + \frac{Re^{-\frac{1}{2}}}{1 + Re^{-\frac{1}{2}}x^{\frac{1}{2}}z}\tau \tag{29}$$

The boundary conditions are

$$\Psi(x, 0) = u(x, 0) = 0 \quad \text{and} \quad u \to 1 \quad \text{as} \quad \eta \to \infty \tag{30}$$

The Keller box [5] method is used to solve (27-30). The Keller box method is a Crank-Nicolson finite difference method, which is second order accurate. Newton's method is used to solve the non-linear set of algebraic equations which result once the equations have been discretised. A uniform grid is used in z. Since the Keller box method involves values only at the present and previous grid points in the streamwise direction, the grid step in x can be changed with no further complications to the method. The streamwise grid step is scaled with $x^{\frac{1}{2}}$ in accordance with the expected development of the boundary layer, so that $\Delta x = x^{\frac{1}{2}}\Delta$.

The initial condition was obtained from (10), (13), and the solution to (14-17). Typical numerical parameters were $z_{max} = 20$, 250 points in z, $\Delta = 0.05$, and $x_0 = 0.01$.

Results

For reference consider a flow with $Re = 10^4$, corresponding e.g. to a cylinder with diameter 1 cm in water with a free stream velocity of 1 m/s. Figure 1 shows the dimensionless skin friction near the leading edge of the cylinder where the Blasius solution should be valid at leading order. Figure 1 shows τ from the numerical solution, the Blasius values and Blasius plus the $O(Re^{-\frac{1}{2}})$ perturbation. Clearly, even at this stage the perturbation is significant, and the Blasius solution alone does not give an accurate estimate of the skin friction.

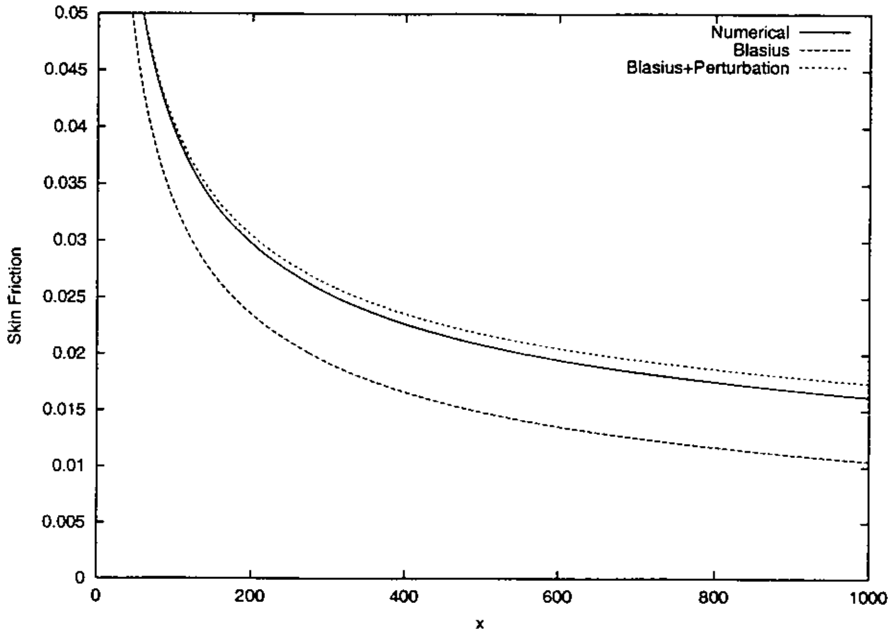

Figure 1: Dimensionless skin friction near the leading edge of the cylinder for $Re = 10^4$

Figure 2 shows the skin friction much further downstream. For very large x, the Blasius values are much too small while the addition of the $O(Re^{-\frac{1}{2}})$ term gives values that are too large. For sufficiently large x the Glauert and Lighthill formula (19) gives excellent results.

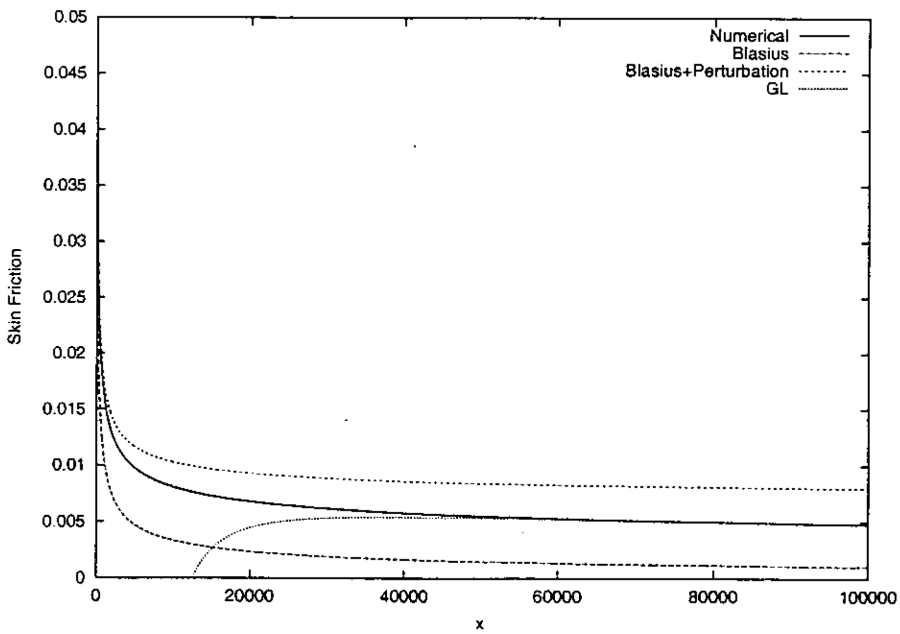

Figure 2: Dimensionless skin friction for $Re = 10^4$

The displacement area is shown in figure 3. This figure displays Δ_1 calculated directly from the numerical solution, using the Blasius solution (22), the expansion valid for $0 < x \ll Re$ (23), and Glauert and Lighthill's expression for large x (24). As expected Δ_1 is smaller than that given using the Blasius profile, and (23) is valid only near the leading edge of the cylinder. Glauert and Lighthill's formula (24) is tending towards the numerical values but only for very large x.

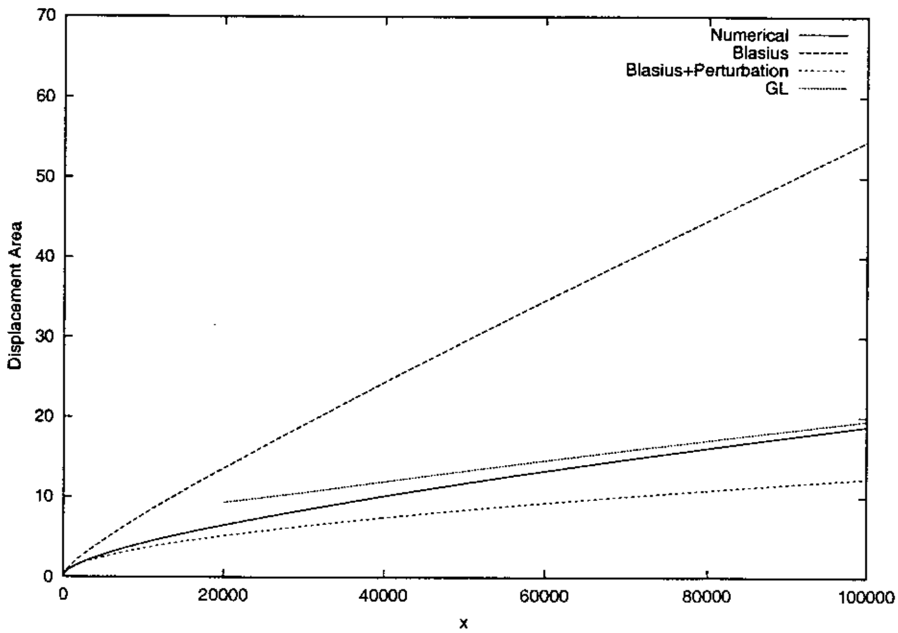

Figure 3: Displacement area for $Re = 10^4$

Perhaps of more interest than the displacement area, which does not give a direct measure of the displacement of the streamlines, is the boundary layer thickness. This is shown in figure 4, along with the Blasius values. The boundary layer thickness has been defined as value of $y = x^{\frac{1}{2}}z$ where $u/U_\infty = 0.99$. The boundary layer is significantly thinner than for the flat plate case, with the difference increasing with x. This is consistent with the higher shear stress in the cylindrical case.

Stability

Flat plate boundary layer flow is one of the cases in which linear stability theory based on a normal mode approach produces a reasonable comparison with experimental results. Hence, for very high values of Re where the flow near the leading edge of the cylinder is given by Blasius flow, linear theory should indicate where the flow first becomes unstable in this case as well. For lower Re or further down the cylinder, the higher values of the wall shear stress and lower values of the displacement area suggest that the flow will be more stable for the cylinder than

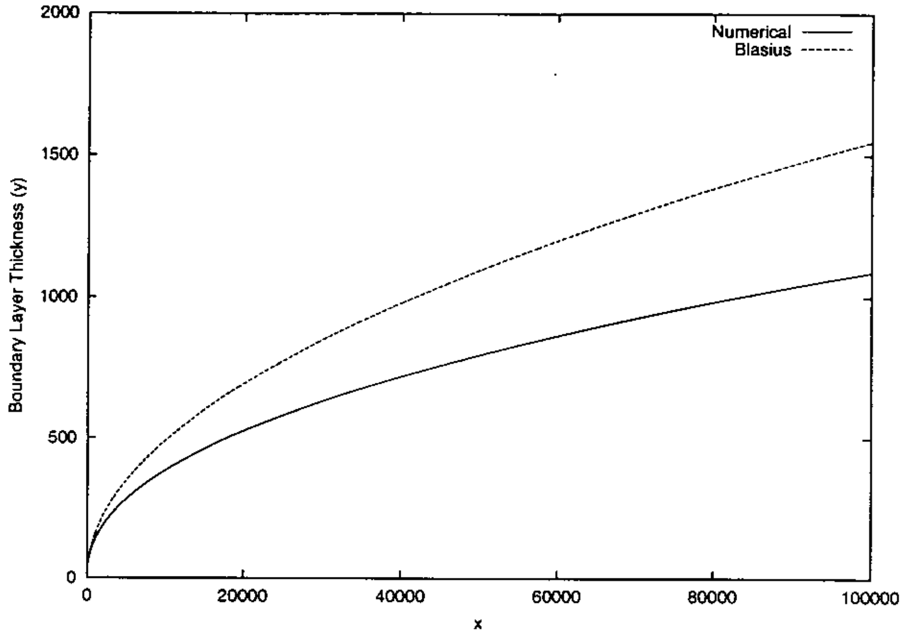

Figure 4: Dimensionless boundary layer thickness for $Re = 10^4$

the flat plate. However, the governing equation for the disturbance is not the same, so this prediction must be treated with caution.

The disturbance to the flow is given by

$$\psi_1 = \phi(r)\exp[i(\alpha x - \omega t)] \tag{31}$$

where ψ_1 is the disturbance streamfunction, $\phi(r)$ its complex amplitude, and α and ω the wave number and frequency of the disturbance. Substituting (31) in the Navier-Stokes equations and linearising produces

$$\left(u - \frac{\omega}{\alpha}\right)(D - \alpha^2)\phi - r\left(\frac{u'}{r}\right)' = \frac{1}{i\alpha Re}(D - \alpha^2)^2\phi \tag{32}$$

where

$$D \equiv \frac{\partial^2}{\partial r^2} - \frac{1}{r}\frac{\partial}{\partial r} \tag{33}$$

Equation (32) is the axisymmetric equivalent of the more familiar Orr-Sommerfeld equation found for two-dimensional flow. Adopting the the boundary layer scaling

$$r = 1 + Re^{-\frac{1}{2}}y, \qquad \alpha = Re^{\frac{1}{2}}\beta \tag{34}$$

(32) becomes

$$(u - c)\left(\frac{\partial^2\phi}{\partial z^2} - \frac{Re^{-\frac{1}{2}}}{r}\frac{\partial\phi}{\partial z} - \beta^2\phi\right) - u'' + \frac{Re^{-\frac{1}{2}}}{r}u' =$$

$$\frac{1}{iR_l\beta}\left[\frac{\partial^4\phi}{\partial z^4} - \frac{2Re^{-\frac{1}{2}}}{r}\frac{\partial^3\phi}{\partial z^3} + \frac{3Re^{-1}}{r^2}\frac{\partial^2\phi}{\partial z^2} - \frac{3Re^{-\frac{3}{2}}}{r^3}\frac{\partial\phi}{\partial z} - 2\beta^2\left(\frac{\partial^2\phi}{\partial z^2} - \frac{Re^{-\frac{1}{2}}}{r}\frac{\partial\phi}{\partial z} - \beta^2\phi\right) + \beta^4\phi\right] \tag{35}$$

where $c = \omega/\alpha$ is the complex wave speed, $R_l = Re^{\frac{1}{2}}$, and the prime on u now refers to $\partial/\partial y$. Clearly for large Re the stability characteristics near the leading edge of the cylinder will be similar to those for the flat plate. Drazin and Reid [6] give the critical values of

$$R_c = 519, \qquad \alpha_c = 0.0304 \tag{36}$$

based on the displacement thickness as the characteristic length. In non-dimensional terms the displacement thickness for Blasius flow is given by

$$\delta_1 = 1.72 x^{\frac{1}{2}} Re^{-\frac{1}{2}} \tag{37}$$

Hence in the scalings used here

$$x_c = \left(\frac{R_c}{1.72}\right)^2 / Re \qquad \text{and} \qquad \beta_c = \frac{\alpha_c}{1.72 x_c^{1/2}} \tag{38}$$

where x_c is the point the flow first becomes unstable.

Calculations were performed for a range of Reynolds numbers. For $Re = 10^5$, which (38) gives $x_c = 0.91$ and $\beta_c = 0.185$, the critical point was found to be at $x_c \approx 0.99$ and $\beta \approx 0.177$. As expected, this is further downstream than for Blasius flow. For $Re = 5 \times 10^4$, (38) gives $x_c = 1.82$ and $\beta_c = 0.131$, while for the cylinder, $x_c \approx 2.18$ with $\beta_c \approx 0.12$.

The gap between the predicted and calculated values of x_c increases as Re decreases. For $Re = 2 \times 10^4$ (38) gives $x_c = 4.55$ and $\beta_c = 0.0828$, while the values from the numerical solution are $x_c \approx 8.02$ and $\beta_c \approx 0.0617$. However, for $Re = 10^4$ no unstable modes were found. Note that at this point the eigenvalue c is consistent with the values for higher Re in that $\Re(c)$ is approximately the same, which indicates that the solution to (35) has not jumped to another branch, i.e. is still obtaining the least stable solution.

Further, even for the higher Re considered here, the flow is unstable only for a finite section of the cylinder, with $\Im(c) > 0$ only for $x_c < x < x_s$, where x_s depends on Re. For $Re = 2 \times 10^4$, $x_s \approx 410$, for $Re = 5 \times 10^4$, $x_s \approx 4800$, and for $Re = 10^5$, $x_s \approx 21211$. In all cases the change back to stable flow is still in the region in which the series with Blasius flow as the leading term might be expected to be valid.

Discussion

Calculations have been performed for the boundary layer on a long thin cylinder, including effects which come from the radial nature of the problem. Near the leading edge of the cylinder a solution can be written as a series which is formally valid for $x \ll Re$, with Blasius flow as the leading term. However, in practice the second term in the series, which is of relative order $(x/Re)^{1/2}$, plays a significant role much closer to the leading edge. In the expression for the skin friction (18), proportional to the leading term, the second term is $2.09(x/Re)^{1/2}$, which equals 0.66 when $x/Re = 1/10$, and 0.21 when $x/Re = 1/100$. Hence, except very close to the leading edge, τ is significantly different from that for Blasius flow. This can be seen clearly in Figure 1 which shows the skin friction near the leading edge for $Re = 10^4$.

Further down the cylinder, when $x \ll Re$, the series solution given by Glauert and Lighthill [4] gives excellent results for the skin friction (Figure 2), but worse agreement for the displacement area (Figure 3).

The boundary layer thickness is lower and the skin friction is higher in the cylinder flow than those for Blasius flow. In general this would suggest that the flow is more stable. This prediction has been borne out, In fact, for flow with $Re = 10^4$ or less the flow is unconditionally stable to linear normal mode disturbances. Physically, the flow would still be expected to become unstable then turbulent along the cylinder as the boundary layer grows in thickness. However, at lower Reynolds numbers there will be no simple, two-dimensional, Tollmein-Schlichting type wave growth/transition scenario. At higher Reynolds numbers, instability when it occurs is further downstream than for Blasius flow, and for the Reynolds numbers investigated in detail, occurs only for a finite length of the cylinder, with the flow becoming stable again when x is still well short of Re. This does not of course imply that the flow will be laminar far downstream. However, with a carefully designed experiment it may be that laminar flow can be maintained much further downstream than with a flat plate (c.f. Poiseuille flow in a pipe as opposed to a channel).

The enhanced stability characteristics over flat plate boundary layer flow are due to a combination of effects. Although the fuller profile found for the cylinder would be expected to be more stable, this is not the full reason. If the velocity profile for the cylinder case with $Re = 10^4$ are used with an Orr-Sommerfeld solver, then unstable modes are found, albeit with the critical point further downstream predicted from (38). Also, if the Blasius profile is used with the cylindrical stability solver, unstable modes are found for $Re = 10^4$. Hence it is both the change in the velocity profile and the effect of the extra term in the stability equation (35) which produces the unconditional stability of the flow when $Re = 10^4$.

Unconditional normal mode linear stability has of course been found with other basic flows. In particular, no unstable modes have been found for Poiseuille flow in a pipe, although this flow is well known to be unstable at sufficiently high Reynolds number.

Finally note that the stabilty of the flow at lower Reynolds numbers rules out some of the standard methods used for in industry for transition prediction, as these commonly rely on empirical correlations of the observed behaviour of basic flows with the linear stability characteristics. In particular, neither the industry standard e^N method or Granvilles method could be used.

Further Work

Considering first a cylinder aligned with the flow, the obvious next step is to extend the numerical modelling to include turbulence. There are a number of ways of increasing complexity that this can be done. The first would be to retain the assumption of boundary layer flow but include a simple turbulence model, such as the Baldwin-Lomax model, along with the standard interaction law as the outer boundary condition. The interaction law couples the outer inviscid flow and inner viscous flow so that the pressure in the boundary layer is not specified but calculated as part of the solution. A more computationally intensive but more satisfactory approach would be to use an incompressible Navier-Stokes solver with one of the standard turbulence models such as the $k - \omega$ model.

Both of these approaches assume axisymmetric flow, and would require reasonable but not excessively large computational resources. The boundary layer approach would involve modifying the boundary layer code used in the present study, while there is an in-house Navier-Stokes solver available at Southampton that could be used for any further work. The aim in both approaches would be to produce estimates of the behaviour of the boundary layer as it develops downstream beyond the laminar stage. Since there should be a similar amount of work involved in these two approaches, the Navier-Stokes one would be prefered.

A more realistic approach would be to calculate the turbulent flow directly, and then calculate the pressure spectrum from the data obtained. There are two main methods that could be used, Large Eddy Simulation (LES) and so-called Direct Numerical Simulations (DNS). The former attempts to calculate the large scale eddies in the flow directly and models the missing, smaller length scale effects through a sub-grid model. The latter makes no approximations, but solves the full Navier-Stokes equations directly. A major advantage of LES is that it can handle flows with much higher Reynolds numbers while DNS should be more accurate/realistic as it should include all effects/length scales, although the maximum Reynolds number flow that can be calculated is limited. Both approaches are feasible but require large computational resources.

Suppose now that the cylinder is not aligned with the flow but exhibits a small amplitude oscillatory motion, with the axis of the cylinder given by

$$r = A\sin(kx - \omega t) \tag{39}$$

where all quantities are in dimensional form. It is assumed here that the oscillation to the cylinder lies in a plane, whereas it could be three-dimensional/helical. However, the basic arguments would stay the same.

If the wave length of the disturbance is L, its wave speed matches the flow speed, and the maximum slope on the cylinder is $1°$ then

$$r = \frac{L}{360}\sin\frac{2\pi}{L}(x - U_\infty t) \tag{40}$$

Suppose now radius of the cylinder is 1 cm, and a typical wavelength is order 100 m, so that $L = 10^4 a$. Then the amplitude of the transverse motion of the cylinder is $O(28a)$, so that, assuming that the growth rate of the boundary layer is still $O((x/Re)^{1/2})$, the motion of the cylinder will not be contained within the boundary layer until $x = O(800Re)$. Hence, although an analysis could be performed with the leading part of the cylinder stationary and the transverse motion sufficiently far downstream that it is contained within the boundary layer, this would require an extremely long cylinder.

The transverse motion of the motion of the cylinder has a Reynolds number based on the peak velocity of

$$R_t = \frac{4\pi}{360} Re = 0.035 Re \tag{41}$$

Hence, in general, given R_t (for example, 350 when $Re = 10^4$), and the size of the transverse motion compared to the thickness of the boundary layer, transverse shedding of the boundary layer/vortices would be expected, and a boundary layer type analysis would not be appropriate, unless the sideways motion of the cylinder occurs only very far downstream .

Consider now the case that the main stream is not aligned with the cylinder, but is inclined at an angle of around to 5°. In this case the velocity normal to the cylinder would be roughly 10% of the free stream velocity. Hence the transverse Reynolds number based on the diameter of the cylinder is sufficiently large that significant cross stream effects could occur. In particular, if the flow was laminar, eddy shedding and a vortex wake might be expected. However, for turbulent flow, much of this secondary motion could be suppressed.

In summary, there are a number of ways this research could proceed, depending largely on the resources available. The most satisfactory would be to perform a DNS or LES study. However, while this is feasible it would require significant resources, not least in terms of the computational facilities required. A more modest approach, which is a obvious first step, would be to use a standard incompressible Navier-Stokes solver with e.g. a $k - \omega$ turbulence model for the flow along the cylinder aligned with the flow. This should provide estimates of the behaviour of the boundary layer as the flow develops downstream, in particular of the growth of the boundary layer and the drag force on the cylinder.

References

[1] R.A. Seban & R. Bond. Skin-friction and heat-transfer characteristics of a laminar boundary layer on a cylinder in axial compressible flow. *J. Aero. Sci.*, **18**, 671-675 (1951).

[2] H.R. Kelly. A note on the laminar boundary layer on a cylinder in axial compressible flow. *J. Aero. Sci.*, **21**, 634 (1954).

[3] K. Stewartson. The asymptotic boundary layer on a circular cylinder in axial incompressible flow. *Q. Appl. Math.*, **13**, 113-122 (1955).

[4] M.B. Glauert & M.J. Lighthill. The axisymmetric boundary layer on a long thin cylinder

[5] P.W. Duck. Viscous flow through unsteady symmetric channels. *J. Fluid Mech.*, **95**, 635-653 (1979).

[6] P.G. Drazin & W.H. Reid. *Hydrodynamic Stability Theory.* CUP (1981).

Boundary Layer Flow on a Long Thin Cylinder

O.R. Tutty W.G. Price

School of Engineering Sciences
University of Southampton
Southampton SO17 1BJ, UK

Introduction

In a classical analysis of the flow in an external boundary layer the pressure gradient is obtained from the inviscid (potential) solution for flow past the body. The simplest example is Blasius flow past a flat plate aligned with the flow in which the pressure gradient is zero. Consider the case of a circular cylinder with the external flow aligned along the cylinders axis. If the cylinder is solid, then the flow will adjust to the presence of the cylinder, generating a nonzero pressure gradient near the nose of the cylinder. However the pressure gradient will decay asymptotically along the cylinder. Alternatively, if fluid is being sucked into the cylinder at the free stream velocity, the pressure gradient will zero from the leading edge.

This problem, of flow developing along a circular cylinder with zero pressure gradient, is the one that will be considered here. There is little reported in the literature on this problem. Seban and Bond [1] give the first three terms in a series solution valid near the leading edge of the cylinder, giving in particular expressions for the shear stress on the surface and the displacement area. Kelly [2] presents different values for some of the coefficients in the Seban and Bond solution. In contrast, Stewartson [3] gives a series solution for very large distances along the cylinder. In [3] it is shown that sufficiently far along the cylinder, the wall shear stress decays logarithmically with distance, rather than than algebraically as is usually found. Glauert and Lighthill [4] considered the flow along the entire cylinder. They developed a similar series solution to Stewartson for the flow far downstream. Also, they developed an approximate solution for flow near the leading edge based on a Pohlhausen method with a logarithmic profile, and have shown that this solution produces reasonable agreement with different series solutions valid near the leading edge and far downstream. Using these solutions they produced a set of recommended curves for quantities such as the displacement area and the skin friction

Here a full numerical solution of the boundary layer problem will be presented and compared with with the previous results.

Formulation

Assuming zero pressure gradient, and the boundary layer equations in polar coordinates (x, r), non-dimensionalised on the cylinder radius, are

$$\frac{\partial u}{\partial x} + \frac{\partial v}{\partial r} + \frac{v}{r} = 0 \tag{1}$$

$$u\frac{\partial u}{\partial x} + v\frac{\partial u}{\partial r} = \frac{1}{Re}\left(\frac{\partial^2 u}{\partial r^2} + \frac{1}{r}\frac{\partial u}{\partial r}\right) \tag{2}$$

where (u, v) are the stream wise and radial velocity components, non-dimensionalised on the free stream velocity U_∞. $Re = U_\infty a/\nu$ is the Reynolds number where ν is the kinematic viscosity.

Introducing the transformation

$$y = (r-1)Re^{\frac{1}{2}}, \qquad v \to Re^{-\frac{1}{2}}v, \tag{3}$$

which incorporates the usual $Re^{-\frac{1}{2}}$ scaling, produces

$$\frac{\partial u}{\partial x} + \frac{\partial v}{\partial y} + \frac{vRe^{-\frac{1}{2}}}{1 + Re^{-\frac{1}{2}}y} = 0 \tag{4}$$

$$u\frac{\partial u}{\partial x} + v\frac{\partial u}{\partial y} = \frac{\partial^2 u}{\partial y^2} + \frac{Re^{-\frac{1}{2}}}{1 + Re^{-\frac{1}{2}}y}\frac{\partial u}{\partial y} \tag{5}$$

with boundary conditions

$$u = v = 0 \quad \text{at} \quad y = 0 \tag{6}$$

$$u \to 1 \quad \text{as} \quad y \to \infty \tag{7}$$

In addition a suitable initial condition must be specified. This will be considered below.

Theoretical Results

From (4-7) it may appear that the leading term in the boundary layer solution will be flat plate Blasius flow, with an $O(Re^{-\frac{1}{2}})$ perturbation. While this is true near the leading edge of the cylinder, further downstream this approximation beaks down. With the Blasius solution, y scales as $x^{\frac{1}{2}}$. Hence the ratio of the terms on the right side of (5) is

$$\frac{Re^{-\frac{1}{2}}}{1 + Re^{-\frac{1}{2}}y}\frac{\partial u}{\partial y}\Big/\frac{\partial^2 u}{\partial y^2} = O\left(\frac{Re^{-\frac{1}{2}}x^{\frac{1}{2}}}{1 + Re^{-\frac{1}{2}}x^{\frac{1}{2}}}\right) \tag{8}$$

Hence when $x = O(Re)$ the terms of the right side are of similar magnitude due to the growth in the boundary layer, and Blasius flow flow will not be the leading term in the solution when the boundary layer thickness becomes comparable with the cylinder radius. Further, at this stage it is also necessary to include the additional term in the continuity equation at leading order.

Here the extra term will be included from the leading edge by adopting the boundary layer equations in the form (4-7). These equations will be solved numerically, using the method outlined below. First, however, the first two term in the series solution for the flow near the leading edge, valid in the region $0 < x \ll Re$, will be presented. Following Seban and Bond, take

$$\eta = Re^{\frac{1}{2}} x^{-\frac{1}{2}} (r^2 - 1)/2, \qquad \xi = Re^{-\frac{1}{2}} x^{\frac{1}{2}} \tag{9}$$

and

$$\psi = Re^{-\frac{1}{2}} x^{\frac{1}{2}} f(\xi, \eta) \tag{10}$$

This gives

$$u = \frac{1}{r}\frac{\partial \psi}{\partial r} = \frac{\partial f}{\partial \eta}, \qquad v = -\frac{1}{r}\frac{\partial \psi}{\partial x} = -\frac{Re^{-\frac{1}{2}} x^{-\frac{1}{2}}}{r}\left[-\eta \frac{\partial f}{\partial \eta} + \frac{\partial}{\partial \xi}(\xi f)\right] \tag{11}$$

The governing equation for f is

$$\frac{\partial}{\partial \eta}\left[(1 + 2\xi\eta)\frac{\partial^2 f}{\partial \eta^2}\right] + \frac{1}{2} f \frac{\partial^2 f}{\partial \eta^2} + \frac{1}{2}\xi\left(\frac{\partial f}{\partial \xi}\frac{\partial^2 f}{\partial \eta^2} + \frac{\partial f}{\partial \eta}\frac{\partial^2 f}{\partial \eta \partial \xi}\right) = 0 \tag{12}$$

Taking

$$f = f_0(\eta) + \xi f_1(\eta) + \dots \tag{13}$$

where it is assumed that $\xi \ll 1$, produces

$$f_0''' + \frac{1}{2} f_0 f_0'' = 0 \tag{14}$$

$$f_1''' + \frac{1}{2} f_0 f_1'' - \frac{1}{2} f_0' f_1' + f_0'' f_1 + 2\eta f_0''' + 2 f_0'' = 0 \tag{15}$$

The boundary conditions are

$$f_0(0) = f_0'(0) = 0 \quad \text{and} \quad f_0' \to 1 \ \text{ as } \ \eta \to \infty \tag{16}$$

$$f_1(0) = f_1'(0) = 0 \quad \text{and} \quad f_1' \to 0 \ \text{ as } \ \eta \to \infty \tag{17}$$

Equation (16) is the Blasius equation. The problems defined by (14-17) are easily solved numerically. The solution give the dimensionless skin friction $\tau = \partial u / \partial y$ as

$$\tau = 0.332 x^{-\frac{1}{2}} + 0.694 Re^{-\frac{1}{2}} + \dots \tag{18}$$

This is essentially the same expression given by Seban and Bond/Kelly [1, 2], but with a small difference in the second coefficient, due presumably to the increased accuracy of the calculations performed here. Equation (18) has the skin friction tending to a constant for large x, although formally it is valid only for $x \ll Re$.

The asymptotic series produced by Glauert and Lighthill [4] for large x gives

$$\tau = \frac{2}{\delta} + \frac{2\gamma}{\delta^2} + \frac{2\gamma^2 - \frac{1}{2}\pi^2 - 4\ln 2}{\delta^3} + O(\delta^{-4}) \tag{19}$$

where $\gamma = 0.5772$ is Euler's constant and $\delta = \ln(4x/Re)$. This formula has τ decaying as x increases, albeit slowly, inversely with $\ln x$. Stewartson [3] produced a similar results, but used $\hat{\delta} = \ln(4x/ReC)$ in place of δ, where $\ln C = \gamma$. Stewartson's formula is

$$\tau = \frac{2}{\hat{\delta}} - \frac{\frac{1}{2}\pi^2 + 4\ln 2}{\hat{\delta}^3} + \ldots + \frac{Re}{2x}\frac{7}{\hat{\delta}} + \ldots \tag{20}$$

Equation (19) can be derived from Stewartson's expression by writing $\hat{\delta} = \delta - \gamma$ and expanding the first two terms in(20) for large x. The Glauert and Lighthill expression for τ is used here as it gives a better comparison with the numerical solutions presented below than Stewartson's formula.

Another of quantity of interest is the "displacement area", which represents the amount by which the fluid in the main stream is displaced by the action the viscous effects in the boundary layer. In two-dimensional flow the displacement thickness gives the distance which the streamlines in the far field are displaced from those of the inviscid flow past the body. However, in cylindrical coordinates, the displacement of the streamlines in away from the surface decays inversely with r due to the expansion in area with r. Hence there is no unique displacement thickness, and the appropriate quantity is the displacement area. In non-dimensional form

$$\Delta_1 = 2\int_1^\infty (1-u) r dr \tag{21}$$

gives the displacement area relative to the cross-sectional area of the cylinder. Substituting the Blasius profile directly into (21) produces

$$\Delta_1 = Re^{-\frac{1}{2}} x^{\frac{1}{2}} \left[3.44 + 4.37 Re^{-\frac{1}{2}} x^{\frac{1}{2}}\right] \tag{22}$$

The solution to (14-17) gives

$$\Delta_1 = Re^{-\frac{1}{2}} x^{\frac{1}{2}} \left[3.442 + 0.143 Re^{-\frac{1}{2}} x^{\frac{1}{2}} + \ldots\right] \tag{23}$$

Equation (23) is valid only for $0 < x \ll Re$. For large x Glauert and Lighthill give

$$\Delta_1 = \frac{4x}{Re}\left[\frac{1}{\delta} + \frac{1 + \gamma + 2\ln 2}{\delta^2} + \ldots\right] \tag{24}$$

Stewartson [3] states that the boundary layer thickness is ultimately of order $(x/Re\hat{\delta})^{\frac{1}{2}}$, consistent with (24). Hence the boundary layer grows at a factor $(\ln x)^{-\frac{1}{2}}$ more slowly than for the flat plate.

Numerical Method

In the original polar coordinates the velocity can be obtained from the streamfunction $\psi(x,r)$ through

$$u = \frac{1}{r}\frac{\partial \psi}{\partial r}, \quad v = -\frac{1}{r}\frac{\partial \psi}{\partial x} \tag{25}$$

In boundary layer coordinates write

$$\psi = Re^{-\frac{1}{2}}\Psi(x,z) \tag{26}$$

where $z = Re^{\frac{1}{2}}x^{-\frac{1}{2}}(r-1)$. The boundary layer equations (4) and (5) can now be written as a system of coupled first order differential equations:

$$u = \frac{x^{-\frac{1}{2}}}{1 + Re^{-\frac{1}{2}}x^{\frac{1}{2}}z}\frac{\partial \Psi}{\partial z} \tag{27}$$

$$\tau = x^{-\frac{1}{2}}\frac{\partial u}{\partial z} \tag{28}$$

$$u\frac{\partial u}{\partial x} - \frac{1}{1 + Re^{-\frac{1}{2}}x^{\frac{1}{2}}z}\frac{\partial \Psi}{\partial x}\tau = x^{-\frac{1}{2}}\frac{\partial \tau}{\partial z} + \frac{Re^{-\frac{1}{2}}}{1 + Re^{-\frac{1}{2}}x^{\frac{1}{2}}z}\tau \tag{29}$$

The boundary conditions are

$$\Psi(x,0) = u(x,0) = 0 \quad \text{and} \quad u \to 1 \quad \text{as} \quad \eta \to \infty \tag{30}$$

The Keller box [5] method is used to solve (27-30). The Keller box method is a Crank-Nicolson finite difference method, which is second order accurate. Newton's method is used to solve the non-linear set of algebraic equations which result once the equations have been discretised. A uniform grid is used in z. Since the Keller box method involves values only at the present and previous grid points in the streamwise direction, the grid step in x can be changed with no further complications to the method. The streamwise grid step is scaled with $x^{\frac{1}{2}}$ in accordance with the expected development of the boundary layer, so that $\Delta x = x^{\frac{1}{2}}\Delta$.

The initial condition was obtained from (10), (13), and the solution to (14-17). Typical numerical parameters were $z_{max} = 20$, 250 points in z, $\Delta = 0.05$, and $x_0 = 0.01$.

Results

For reference consider a flow with $Re = 10^4$, corresponding e.g. to a cylinder with diameter 1 *cm* in water with a free stream velocity of 1 *m/s*. Figure 1 shows the dimensionless skin friction near the leading edge of the cylinder where the Blasius solution should be valid at leading order. Figure 1 shows τ from the numerical solution, the Blasius values and Blasius plus the $O(Re^{-\frac{1}{2}})$ perturbation. Clearly, even at this stage the perturbation is significant, and the Blasius solution alone does not give an accurate estimate of the skin friction.

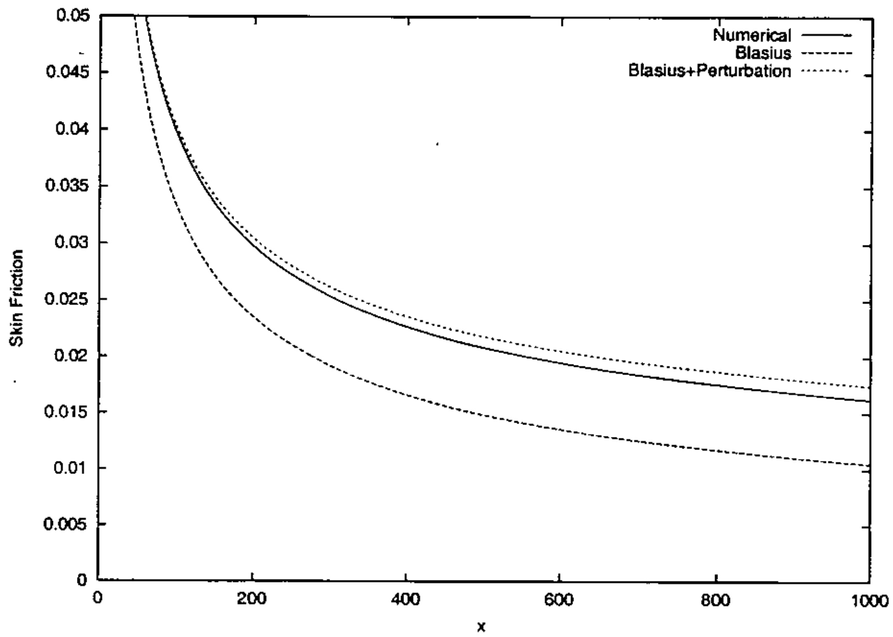

Figure 1: Dimensionless skin friction near the leading edge of the cylinder for $Re = 10^4$

Figure 2 shows the skin friction much further downstream. For very large x, the Blasius values are much too small while the addition of the $O(Re^{-\frac{1}{2}})$ term gives values that are too large. For sufficiently large x the Glauert and Lighthill formula (19) gives excellent results.

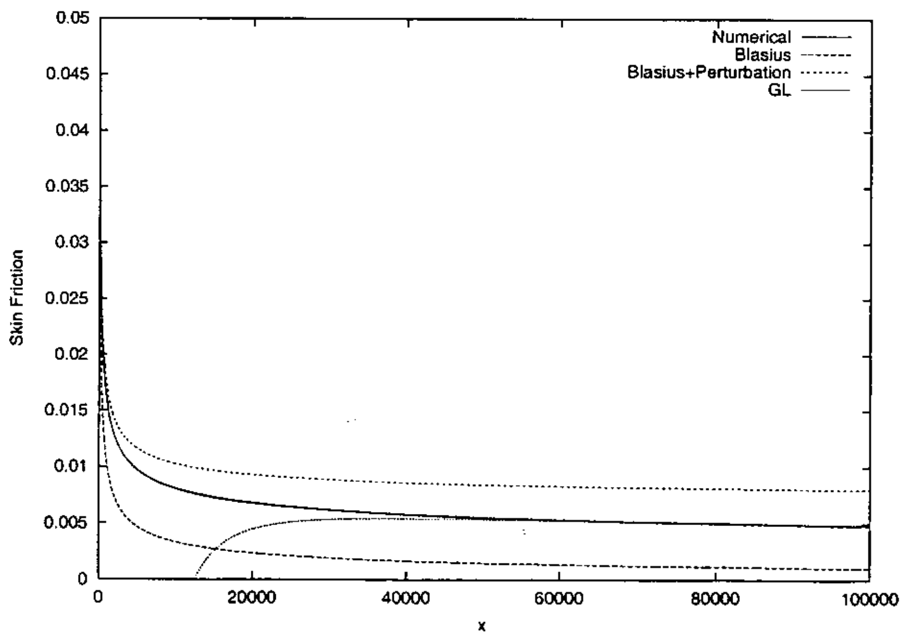

Figure 2: Dimensionless skin friction for $Re = 10^4$

The displacement area is shown in figure 3. This figure displays Δ_1 calculated directly from the numerical solution, using the Blasius solution (22), the expansion valid for $0 < x \ll Re$ (23), and Glauert and Lighthill's expression for large x (24). As expected Δ_1 is smaller than that given using the Blasius profile, and (23) is valid only near the leading edge of the cylinder. Glauert and Lighthill's formula (24) is tending towards the numerical values but only for very large x.

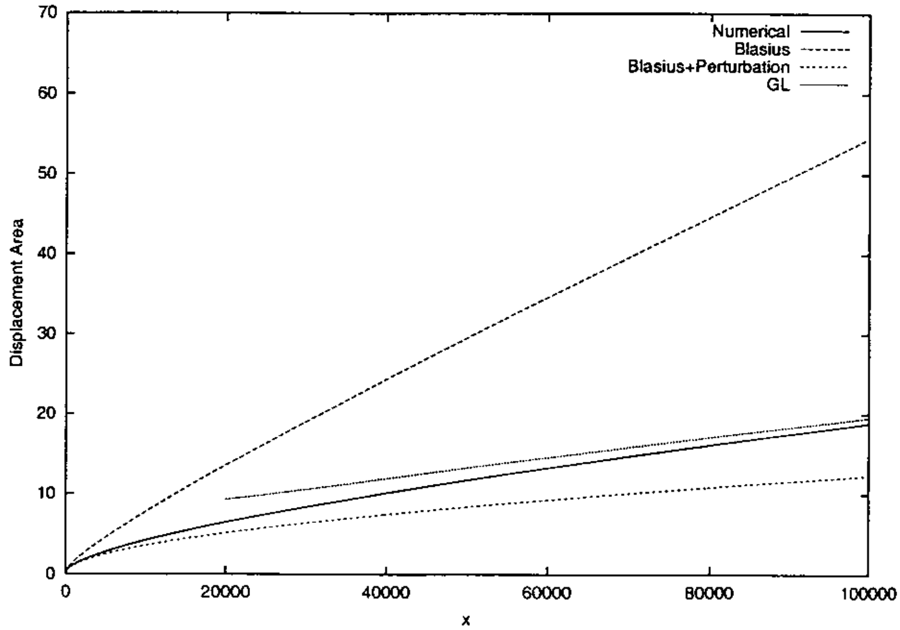

Figure 3: Displacement area for $Re = 10^4$

Perhaps of more interest than the displacement area, which does not give a direct measure of the displacement of the streamlines, is the boundary layer thickness. This is shown in figure 4, along with the Blasius values. The boundary layer thickness has been defined as value of $y = x^{\frac{1}{2}}z$ where $u/U_\infty = 0.99$. The boundary layer is significantly thinner than for the flat plate case, with the difference increasing with x. This is consistent with the higher shear stress in the cylindrical case.

Stability

Flat plate boundary layer flow is one of the cases in which linear stability theory based on a normal mode approach produces a reasonable comparison with experimental results. Hence, for very high values of Re where the flow near the leading edge of the cylinder is given by Blasius flow, linear theory should indicate where the flow first becomes unstable in this case as well. For lower Re or further down the cylinder, the higher values of the wall shear stress and lower values of the displacement area suggest that the flow will be more stable for the cylinder than

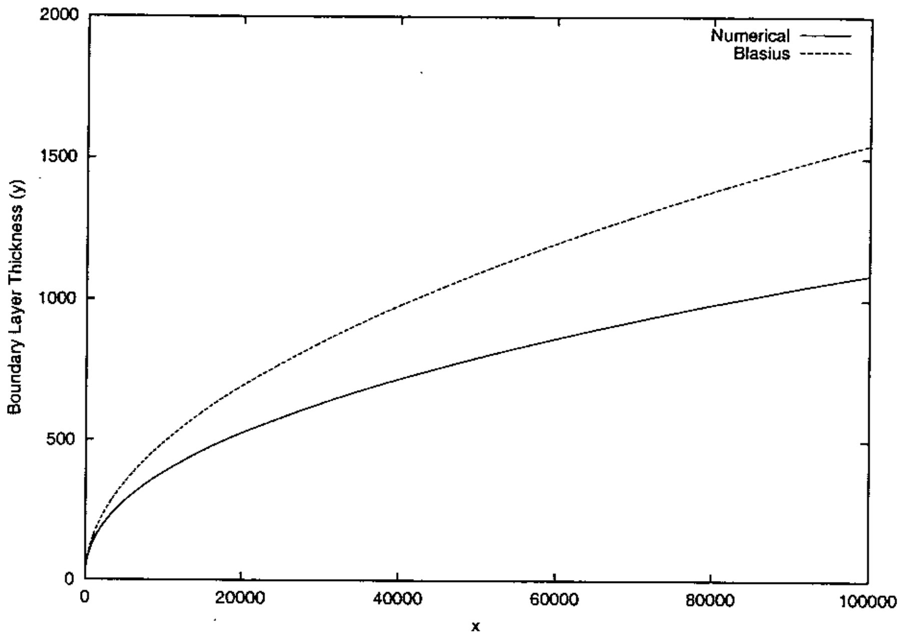

Figure 4: Dimensionless boundary layer thickness for $Re = 10^4$

the flat plate. However, the governing equation for the disturbance is not the same, so this prediction must be treated with caution.

The disturbance to the flow is given by

$$\psi_1 = \phi(r)\exp[i(\alpha x - \omega t)] \tag{31}$$

where ψ_1 is the disturbance streamfunction, $\phi(r)$ its complex amplitude, and α and ω the wave number and frequency of the disturbance. Substituting (31) in the Navier-Stokes equations and linearising produces

$$\left(u - \frac{\omega}{\alpha}\right)(D - \alpha^2)\phi - r\left(\frac{u'}{r}\right)' = \frac{1}{i\alpha Re}(D - \alpha^2)^2\phi \tag{32}$$

where

$$D \equiv \frac{\partial^2}{\partial r^2} - \frac{1}{r}\frac{\partial}{\partial r} \tag{33}$$

Equation (32) is the axisymmetric equivalent of the more familiar Orr-Sommerfeld equation found for two-dimensional flow. Adopting the the boundary layer scaling

$$r = 1 + Re^{-\frac{1}{2}}y, \qquad \alpha = Re^{\frac{1}{2}}\beta \tag{34}$$

(32) becomes

$$(u - c)\left(\frac{\partial^2\phi}{\partial z^2} - \frac{Re^{-\frac{1}{2}}}{r}\frac{\partial\phi}{\partial z} - \beta^2\phi\right) - u'' + \frac{Re^{-\frac{1}{2}}}{r}u' =$$

$$\frac{1}{iR_l\beta}\left[\frac{\partial^4\phi}{\partial z^4} - \frac{2Re^{-\frac{1}{2}}}{r}\frac{\partial^3\phi}{\partial z^3} + \frac{3Re^{-1}}{r^2}\frac{\partial^2\phi}{\partial z^2} - \frac{3Re^{-\frac{3}{2}}}{r^3}\frac{\partial\phi}{\partial z} - 2\beta^2\left(\frac{\partial^2\phi}{\partial z^2} - \frac{Re^{-\frac{1}{2}}}{r}\frac{\partial\phi}{\partial z} - \beta^2\phi\right) + \beta^4\phi\right] \tag{35}$$

where $c = \omega/\alpha$ is the complex wave speed, $R_l = Re^{\frac{1}{2}}$, and the prime on u now refers to $\partial/\partial y$.

Clearly for large Re the stability characteristics near the leading edge of the cylinder will be similar to those for the flat plate. Drazin and Reid [6] give the critical values of

$$R_c = 519, \qquad \alpha_c = 0.0304 \tag{36}$$

based on the displacement thickness as the characteristic length. In non-dimensional terms the displacement thickness for Blasius flow is given by

$$\delta_1 = 1.72 x^{\frac{1}{2}} Re^{-\frac{1}{2}} \tag{37}$$

Hence in the scalings used here

$$x_c = \left(\frac{R_c}{1.72}\right)^2 / Re \qquad \text{and} \qquad \beta_c = \frac{\alpha_c}{1.72 x_c^{1/2}} \tag{38}$$

where x_c is the point the flow first becomes unstable.

Calculations were performed for a range of Reynolds numbers. For $Re = 10^5$, which (38) gives $x_c = 0.91$ and $\beta_c = 0.185$, the critical point was found to be at $x_c \approx 0.99$ and $\beta \approx 0.177$. As expected, this is further downstream than for Blasius flow. For $Re = 5 \times 10^4$, (38) gives $x_c = 1.82$ and $\beta_c = 0.131$, while for the cylinder, $x_c \approx 2.18$ with $\beta_c \approx 0.12$.

The gap between the predicted and calculated values of x_c increases as Re decreases. For $Re = 2 \times 10^4$ (38) gives $x_c = 4.55$ and $\beta_c = 0.0828$, while the values from the numerical solution are $x_c \approx 8.02$ and $\beta_c \approx 0.0617$. However, for $Re = 10^4$ no unstable modes were found. Note that at this point the eigenvalue c is consistent with the values for higher Re in that $\Re(c)$ is approximately the same, which indicates that the solution to (35) has not jumped to another branch, i.e. is still obtaining the least stable solution.

Further, even for the higher Re considered here, the flow is unstable only for a finite section of the cylinder, with $\Im(c) > 0$ only for $x_c < x < x_s$, where x_s depends on Re. For $Re = 2 \times 10^4$, $x_s \approx 410$, for $Re = 5 \times 10^4$, $x_s \approx 4800$, and for $Re = 10^5$, $x_s \approx 21211$. In all cases the change back to stable flow is still in the region in which the series with Blasius flow as the leading term might be expected to be valid.

Discussion

Calculations have been performed for the boundary layer on a long thin cylinder, including effects which come from the radial nature of the problem. Near the leading edge of the cylinder a solution can be written as a series which is formally valid for $x \ll Re$, with Blasius flow as the leading term. However, in practice the second term in the series, which is of relative order $(x/Re)^{1/2}$, plays a significant role much closer to the leading edge. In the expression for the skin friction (18), proportional to the leading term, the second term is $2.09(x/Re)^{1/2}$, which equals 0.66 when $x/Re = 1/10$, and 0.21 when $x/Re = 1/100$. Hence, except very close to the leading edge, τ is significantly different from that for Blasius flow. This can be seen clearly in Figure 1 which shows the skin friction near the leading edge for $Re = 10^4$.

Further down the cylinder, when $x \ll Re$, the series solution given by Glauert and Lighthill [4] gives excellent results for the skin friction (Figure 2), but worse agreement for the displacement area (Figure 3).

The boundary layer thickness is lower and the skin friction is higher in the cylinder flow than those for Blasius flow. In general this would suggest that the flow is more stable. This prediction has been borne out, In fact, for flow with $Re = 10^4$ or less the flow is unconditionally stable to linear normal mode disturbances. Physically, the flow would still be expected to become unstable then turbulent along the cylinder as the boundary layer grows in thickness. However, at lower Reynolds numbers there will be no simple, two-dimensional, Tollmein-Schlichting type wave growth/transition scenario. At higher Reynolds numbers, instability when it occurs is further downstream than for Blasius flow, and for the Reynolds numbers investigated in detail, occurs only for a finite length of the cylinder, with the flow becoming stable again when x is still well short of Re. This does not of course imply that the flow will be laminar far downstream. However, with a carefully designed experiment it may be that laminar flow can be maintained much further downstream than with a flat plate (c.f. Poiseuille flow in a pipe as opposed to a channel).

The enhanced stability characteristics over flat plate boundary layer flow are due to a combination of effects. Although the fuller profile found for the cylinder would be expected to be more stable, this is not the full reason. If the velocity profile for the cylinder case with $Re = 10^4$ are used with an Orr-Sommerfeld solver, then unstable modes are found, albeit with the critical point further downstream predicted from (38). Also, if the Blasius profile is used with the cylindrical stability solver, unstable modes are found for $Re = 10^4$. Hence it is both the change in the velocity profile and the effect of the extra term in the stability equation (35) which produces the unconditional stability of the flow when $Re = 10^4$.

Unconditional normal mode linear stability has of course been found with other basic flows. In particular, no unstable modes have been found for Poiseuille flow in a pipe, although this flow is well known to be unstable at sufficiently high Reynolds number.

Finally note that the stabilty of the flow at lower Reynolds numbers rules out some of the standard methods used for in industry for transition prediction, as these commonly rely on empirical correlations of the observed behaviour of basic flows with the linear stability characteristics. In particular, neither the industry standard e^N method or Granvilles method could be used.

Further Work

Considering first a cylinder aligned with the flow, the obvious next step is to extend the numerical modelling to include turbulence. There are a number of ways of increasing complexity that this can be done. The first would be to retain the assumption of boundary layer flow but include a simple turbulence model, such as the Baldwin-Lomax model, along with the standard interaction law as the outer boundary condition. The interaction law couples the outer inviscid flow and inner viscous flow so that the pressure in the boundary layer is not specified but calculated as part of the solution. A more computationally intensive but more satisfactory approach would be to use an incompressible Navier-Stokes solver with one of the standard turbulence models such as the $k - \omega$ model.

Both of these approaches assume axisymmetric flow, and would require reasonable but not excessively large computational resources. The boundary layer approach would involve modifying the boundary layer code used in the present study, while there is an in-house Navier-Stokes solver available at Southampton that could be used for any further work. The aim in both approaches would be to produce estimates of the behaviour of the boundary layer as it develops downstream beyond the laminar stage. Since there should be a similar amount of work involved in these two approaches, the Navier-Stokes one would be prefered.

A more realistic approach would be to calculate the turbulent flow directly, and then calculate the pressure spectrum from the data obtained. There are two main methods that could be used, Large Eddy Simulation (LES) and so-called Direct Numerical Simulations (DNS). The former attempts to calculate the large scale eddies in the flow directly and models the missing, smaller length scale effects through a sub-grid model. The latter makes no approximations, but solves the full Navier-Stokes equations directly. A major advantage of LES is that it can handle flows with much higher Reynolds numbers while DNS should be more accurate/realistic as it should include all effects/length scales, although the maximum Reynolds number flow that can be calculated is limited. Both approaches are feasible but require large computational resources.

Suppose now that the cylinder is not aligned with the flow but exhibits a small amplitude oscillatory motion, with the axis of the cylinder given by

$$r = A\sin(kx - \omega t) \tag{39}$$

where all quantities are in dimensional form. It is assumed here that the oscillation to the cylinder lies in a plane, whereas it could be three-dimensional/helical. However, the basic arguments would stay the same.

If the wave length of the disturbance is L, its wave speed matches the flow speed, and the maximum slope on the cylinder is $1°$ then

$$r = \frac{L}{360}\sin\frac{2\pi}{L}(x - U_\infty t) \tag{40}$$

Suppose now radius of the cylinder is 1 cm, and a typical wavelength is order 100 m, so that $L = 10^4 a$. Then the amplitude of the transverse motion of the cylinder is $O(28a)$, so that, assuming that the growth rate of the boundary layer is still $O((x/Re)^{1/2})$, the motion of the cylinder will not be contained within the boundary layer until $x = O(800Re)$. Hence, although an analysis could be performed with the leading part of the cylinder stationary and the transverse motion sufficiently far downstream that it is contained within the boundary layer, this would require an extremely long cylinder.

The transverse motion of the motion of the cylinder has a Reynolds number based on the peak velocity of

$$R_t = \frac{4\pi}{360} Re = 0.035Re \tag{41}$$

Hence, in general, given R_t (for example, 350 when $Re = 10^4$), and the size of the transverse motion compared to the thickness of the boundary layer, transverse shedding of the boundary layer/vortices would be expected, and a boundary layer type analysis would not be appropriate, unless the sideways motion of the cylinder occurs only very far downstream .

Consider now the case that the main stream is not aligned with the cylinder, but is inclined at an angle of around to 5°. In this case the velocity normal to the cylinder would be roughly 10% of the free stream velocity. Hence the transverse Reynolds number based on the diameter of the cylinder is sufficiently large that significant cross stream effects could occur. In particular, if the flow was laminar, eddy shedding and a vortex wake might be expected. However, for turbulent flow, much of this secondary motion could be suppressed.

In summary, there are a number of ways this research could proceed, depending largely on the resources available. The most satisfactory would be to perform a DNS or LES study. However, while this is feasible it would require significant resources, not least in terms of the computational facilities required. A more modest approach, which is a obvious first step, would be to use a standard incompressible Navier-Stokes solver with e.g. a $k - \omega$ turbulence model for the flow along the cylinder aligned with the flow. This should provide estimates of the behaviour of the boundary layer as the flow develops downstream, in particular of the growth of the boundary layer and the drag force on the cylinder.

References

[1] R.A. Seban & R. Bond. Skin-friction and heat-transfer characteristics of a laminar boundary layer on a cylinder in axial compressible flow. *J. Aero. Sci.*, **18**, 671-675 (1951).

[2] H.R. Kelly. A note on the laminar boundary layer on a cylinder in axial compressible flow. *J. Aero. Sci.*, **21**, 634 (1954).

[3] K. Stewartson. The asymptotic boundary layer on a circular cylinder in axial incompressible flow. *Q. Appl. Math.*, **13**, 113-122 (1955).

[4] M.B. Glauert & M.J. Lighthill. The axisymmetric boundary layer on a long thin cylinder

[5] P.W. Duck. Viscous flow through unsteady symmetric channels. *J. Fluid Mech.*, **95**, 635-653 (1979).

[6] P.G. Drazin & W.H. Reid. *Hydrodynamic Stability Theory*. CUP (1981).